Passive self-aligning of a floating offshore wind turbine

Passive self-aligning of a floating offshore wind turbine

S Netzband, CW Schulz, M Abdel-Maksoud

Institute for Fluid Dynamics and Ship Theory, Hamburg University of Technology, Am Schwarzenberg-Campus 1, 21073 Hamburg, Germany

E-mail: stefan.netzband@tuhh.de

Abstract. The development of floating offshore wind turbines opens the way for various new design types, and the platform, tower and turbine can benefit from its floating foundation. Self-aligning platforms, where the entire structure follows the wind direction are a promising concept. A single point mooring with turret system allows for free rotation around the vertical axis. Aerodynamic forces of rotor and tower induce the self-aligning moment. In the present study, the operating principle of a passive platform design with airfoil-shaped tower and downwind rotor is analyzed under steady conditions using a boundary element method (BEM). Rotor cone angle and the tower dimensions have a major influence on the yawing moment. They must be large enough to dominate the hydrodynamic forces induced by seaway and current. The passive self-aligning capability is shown in an integrated simulation for various current velocities and wind-current offset angles.

1. Introduction

The development of floating offshore wind turbines has rapidly increased in recent years, along with new platform designs. Most of these designs have replaced the fixed foundation of offshore wind turbines with a floating structure, while keeping the same towers and turbines in order to avoid large-scale changes. However, other platform designs have attempted to take advantage of the floating condition by introducing a variety of self-aligning platform types, in which the aerodynamic forces passively align the platform in the wind. In these designs, a single point mooring (SPM) is essential as it allows for free rotation, which also means that a yaw bearing is no longer necessary on the tower top. The advantages of this are a simplification of the design with defined load directions and a lower center of gravity, which allows lower structural mass and a simplified installation because of one single connection point to the anchor system and power cable.

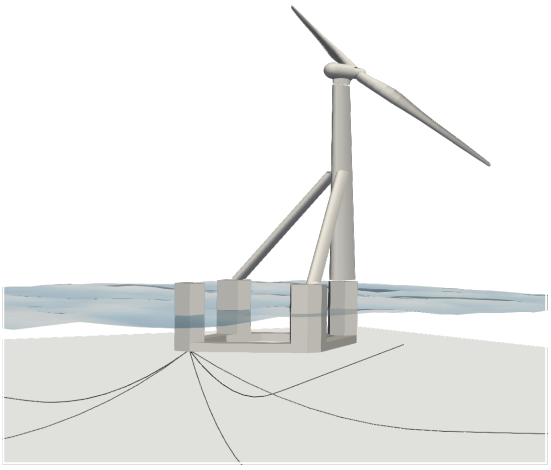

Figure 1. The self-aligning semi-submersible platform with single point mooring and downwind rotor.

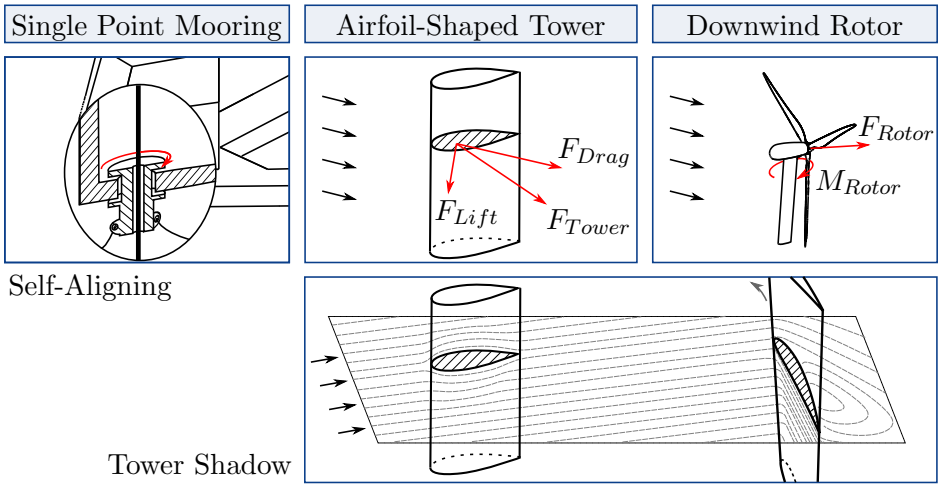

Figure 2. Illustration of the self-aligning principle and tower shadow effect.

This paper presents the analysis of the passively yawing semi-submersible platform SelfAligner as seen in Figure 1. It consists of four columns mounted on a large rhomb-shaped base plate. The SPM is housed in one column and the tower is based on the opposite column. Two struts on the lateral columns support the tower on the lower half. All parts of the tower have an airfoil shape which reduces tower shadow and induces a self-aligning moment when the platform is not aligned with the wind. A 6MW downwind turbine with two blades is mounted on top of the tower. Figure 2 illustrates the key points of the design, which allows the platform to passively follow the wind direction. No active system like a ballast water system with pumps is needed.

The analysis has been carried out with an unsteady three-dimensional first-order panel method for both aerodynamic and hydrodynamic domain. A lumped mass mooring model is used for the line forces. A description of the method used in this project is given below in a short version but has been published in more detail [1, 2].

A first objective is to acquire a clear understanding of the aligning forces induced by the rotor. Aerodynamic force direction and yawing moment change with wind speed and orientation. The cone angle has a major influence on the self aligning forces and enables improvements by structural modifications. Its influence on the yaw stability has been shown for bottom fixed downwind turbines in experiments [3–5] and simulations [6]. They all have determined an increased yaw stability with increasing downwind cone. Beyond the yaw stability, rotor forces on self-aligning platforms are required to turn the entire platform into the wind direction. A study of the misalignment under different wind and sea-current velocities as well as offset angles has been carried out to determine the misalignment angles as well as turbine power loss. It is also used to calculate the influence of the airfoil-shaped tower structure on the self-alignment.

2. Method

The boundary element method *pan*MARE has been used for various simulations in the field of ship and offshore simulations. Originally it was developed to calculate the flow field around ship propellers [7, 8]. Later *pan*MARE was used to estimate the dynamic behavior of floating bodies [9]. In recent years it was adapted to simulate the motion behavior of floating offshore wind turbines [1, 2]. *pan*MARE is capable of estimating the aerodynamic forces and moments as well as the hydrodynamic loading within two separate domains while using one single method. It is a time domain method where the flow field is solved at each time step. Body shapes and rotor wake are discretized by first-order panels.

With the assumption of an incompressible, irrotational and inviscid fluid, it is possible to describe the flow field by the gradient of a scalar potential Φ. The continuity equation can then be reduced to the Laplace equation:

$$\Delta\Phi = 0 \tag{1}$$

The potential Φ is decomposed into several parts $\Phi = \Phi_{ext} + \Phi_{ind} + \Phi_{wave}$. By an external potential Φ_{ext}, the uniform inflow is applied, which is either the current or wind. The induced potential Φ_{ind} describes the influence of all panels in the domain.

Body panels have a source strength σ and a doublet strength μ. The Dirichlet boundary condition is applied based on the idea of a constant potential $\Phi = 0$ inside a closed body which leads to two conditions for the source and doublet strength for each panel.

$$\begin{aligned} \sigma &= (\vec{v}_{ext} + \nabla\Phi_{wave} - \vec{v}_m) \cdot \vec{n} \\ \frac{1}{4\pi}\int_{body+wake} \mu \frac{\delta}{\delta\vec{n}} dA - \frac{1}{4\pi}\int_{body} \sigma \frac{1}{r} dA &= 0 \end{aligned} \tag{2}$$

The remaining values are the panel normal outward direction $\vec{n}$, the distance between the evaluation point and panel center r, the panel area A and the panel motion velocity in global coordinates $\vec{v}_m$. Detailed information on how to obtain a closed set of equations and about the solving procedure are given by Katz and Plotkin [10].

The wake of lifting bodies is discretized by wake panels with a doublet strength μ to consider the circulation around the body. A row of new wake panels is shed from the trailing edge at each time step between the trailing edge and the first wake panels. Their doublet strength is determined by the upper and lower body panel using the Kutta condition.

$$\mu_{wakepanel} = \mu_{upper} - \mu_{lower} \tag{3}$$

In the following time steps, the wake panel deforms freely and is transported downstream by the flow. With increasing distance the influence on the rotor decreases. Hence, wake panels are removed after a certain number of time steps. In the present case the rotor blades are the only lifting bodies with wake.

A wave potential Φ_{wave} is present in the hydrodynamic domain only. Irregular waves are applied by a superposition of regular waves with a potential depending on the position $\vec{r}$ and time t.

$$\Phi_{wave}(\vec{r}, t) = -\zeta_a \frac{2\pi}{kT} \frac{\cosh(k(z-d))}{\sinh(kd)} \mathrm{Re}\{i\mathrm{e}^{i(-\omega t + k\bar{x} + \epsilon)}\} \tag{4}$$

The characterizing values of the wave are the amplitude ζ_a, angular wave frequency ω, wave number k, phase shift ϵ and water depth d. The distance $\bar{x}$ is given by horizontal length of $\vec{r}$ in wave propagation direction. Panels which are above the local wave elevation are suppressed at each solve step to eliminate their influence on the flow field. It is important to note here that no special treatment of the water surface was undertaken. Hence, radiation and diffraction effects are not accounted for, as described in the previous paper [1].

The fluid velocity is given by the gradient of the potential:

$$\vec{v} = \vec{v}_{ext} + \nabla\Phi_{ind} + \nabla\Phi_{wave}\,. \tag{5}$$

On each panel the pressure is calculated using Bernoulli's equation for the unsteady flow:

$$\frac{p}{\rho} = \vec{g}\vec{r} - \frac{1}{2}\vec{v}_{rel}^2 - \frac{\delta\Phi}{\delta t} + \frac{1}{2}\vec{v}_m^2\,, \tag{6}$$

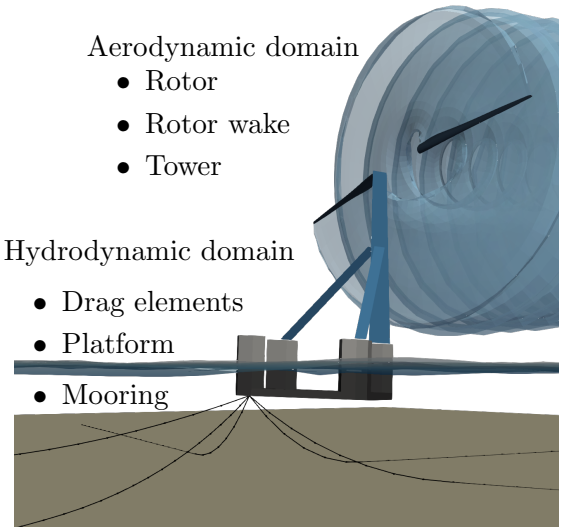

Figure 3. Simulation domains.

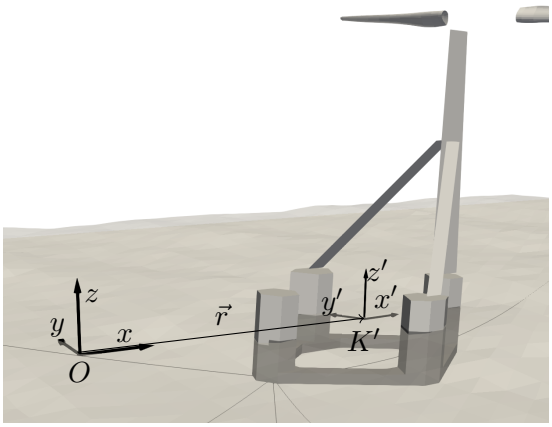

Figure 4. Global and local coordinate systems.

with the gravitational acceleration $\vec{g}$, the panel centre $\vec{r}$ and its relative velocity $\vec{v}_{rel}$ and fluid density ρ. Based on ITTC-1957 an additional friction force is estimated using the streamline at the panel center.

Additional force elements are implemented in order to estimate forces that are not covered by potential flow. These elements are based on direction-dependent lift and drag coefficients which have been obtained in advance, similar to the idea of the blade element theory. The elements evaluate the local fluid velocity at their center points to calculate the induced forces. However, they to not have any influence on the flow field. In the present case force elements are used to consider the hull drag of the platform and the aerodynamic forces on the tower.

A lumped mass method [11] is implemented in order to determine to the dynamic line forces of the mooring. It consists of mass nodes connected by spring-damper elements. Inertia and fluid forces are concentrated on the nodes. The solving procedure of the mooring model is deeply integrated in the general solving routine and follows the steps of the hydrodynamic domain.

A six degrees of freedom solver is used to predict the motion of the platform. Structural deformation such as blade deflection or tower bending is not covered. Only an additional degree of freedom was given to the rotor to rotate freely. The acceleration of the platform is calculated by solving the Newton-Euler equations. A fourth-order Runge-Kutta (RK4) method is used to obtain the velocity and transformation. All models, aerodynamic, hydrodynamic and mooring, are synchronized within each sub-step during of the RK4 scheme.

Operational conditions are limited to partial turbine load due to a missing blade pitch controller. The turbine has not been shutdown at higher misalignment angles. A shutdown could be reasonable to avoid high fatigue loads but this study focuses on the passive alignment of the platform to the wind.

3. Model setup

A global overview of the setup is given in Figure 3. It is identical to the setup in the previous work [2]. The aerodynamic domain contains the rotor, its wake and the tower. Platform and mooring are within the hydrodynamic domain. Densities and global properties are given in Table 1. The location of the total center of gravity (COG) is shifted towards the turret buoy to reduce the backward trim angle during turbine operation. A very small sidewise shift is applied to counteract the rotor torque when operating at nominal conditions. Figure 4 shows the local

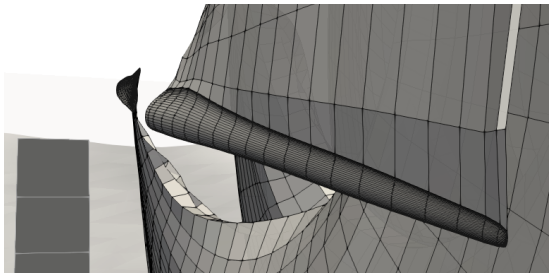

Figure 5. Rotor grid.

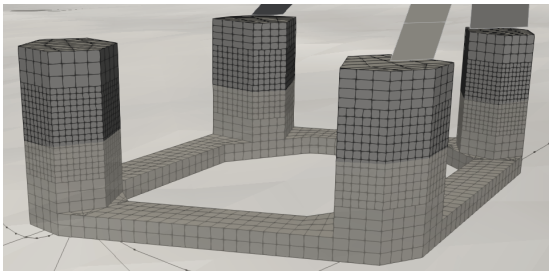

Figure 6. Platform grid.

Table 1. Global parameter.

Property	Value
Densities ρ_{Water}	$1025\,\mathrm{kg\,m^{-3}}$
ρ_{Air}	$1.24\,\mathrm{kg\,m^{-3}}$
Gravitation g	$9.81\,\mathrm{m\,s^{-2}}$
Total mass	7879 t
COG lengthwise shift	−0.07 m
sidewise shift	0.07 m
below SWL	−2.4 m

Table 2. Basic rotor information.

Property	Value
Number of blades	2
Rotor diameter	140 m
Nominal rotor speed	$13.6\,\mathrm{min^{-1}}$
Principle	downwind
Hub height	90 m
Cone angle	9.0° (downwind)

Table 3. Platform drag coefficient.

Body	Angle of attack α 0°	90°
Beams	0.75	1.5
Fore & aft column	1.2	1.2
Lateral column	0.8	1.2

Table 4. Wind velocities and seaway.

Wind velocity v_{Air} [$\mathrm{m\,s^{-1}}$]	Significant wave height H_S [m]	Peak wave period T_p [s]
5.2	1.2	6.72
7.9	1.88	7.41
10.5	2.85	8.38
11.8	3.44	8.96

coordinate system K' at the COG and its relation to the global Cartesian coordinate system O. Wind and current were introduced with a constant fluid velocity v_{ext}.

Basic information about the rotor are given in Table 2. It has a cone angle of 9° in downwind direction. Each blade was discretized using 1260 body panels in rectangular grid and with refinements at the leading and trailing edge and blade tip, see Figure 5. The wake of each blade has the same spanwise distribution and was represented by 4000 panels. Only the lifting part of the blade is represented by panels. The blade root, with its circular shape, has not been included in the simulation. A symmetry condition was placed at still water level (SWL) to account for ground effects in the aerodynamic domain.

The tower and two struts have a NACA 0035 airfoil shape with chord lengths of 8 m to 12 m (top to bottom) and 6 m, respectively. As BEM has limitations regarding the maximum thickness, 2D simulations of NACA 0035 airfoils have shown large inaccuracies of lift and drag forces using *pan*MARE. Hence, the tower is represented by 30 force elements to cover the forces more precisely. Lift and drag coefficients are based on experimental results by Sarraf et al. [12]. Data are available for an angle of attack between −35° to 35°. Therefore, the simulation of the

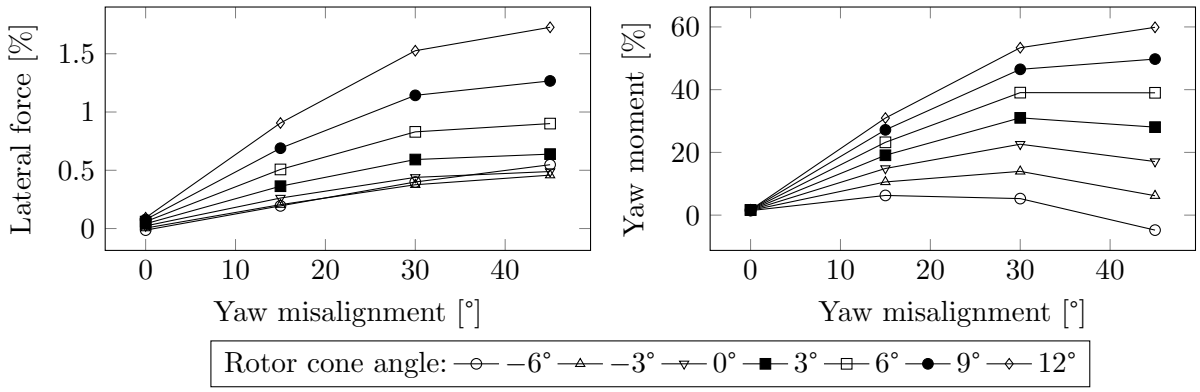

Figure 7. Mean values of lateral rotor force and yaw moment at tower top relativized to rotor thrust and torque.

platform is limited to misalignment angles below 35°.

The platform is discretized by 4492 body panels with a refinement in the region of the water surface, see Figure 6. Viscous effects have a major influence on forces induced by the sea current. In total 60 force elements are spread along the beam and column structure in order to include these forces. The drag coefficients of the different shapes are given in Table 3 for angles of attack of 0° and 90°. These values are based on the results of RANS simulations for the full-scale. A linear interpolation is performed between 0° and 90°.

The mooring system consists of five mooring lines circularly distributed around the turret buoy. All fairleads are connected at the same point in the simulation model. Hence, no yaw moment can be induced by the mooring. Each line has a length of 350 m and is discretized by 30 elements. The water depth is set to 40 m.

The environmental conditions for four wind speeds are given in Table 4. A JONSWAP spectrum is defined by the significant wave height and peak period using an enhancement factor of 3.3. In *pan*MARE, irregulare waves are represented by a superposition of regular waves. In this case only long-crested waves are applied with its propagation direction equal to the current direction. This might be unusual for wind-induced waves but was presumed as a worst-case scenario.

All simulations were carried out in time-domain until the mean values showed steady behavior.

4. Results

Three sets of simulations have been carried out to obtain the results presented in this paper. At first only the rotor is simulated with different rotor cone angles to obtain its influence on the self-aligning moment. In a second step, platform, tower and rotor forces are computed separately under static conditions. The steady motion state on condition of free movement with platform, rotor and mooring system is simulated simultaneously in the third step. In all sets the model setup and discretization are similar, as described above.

4.1. Rotor cone angle influence on self-aligning moments

In the first set, the aerodynamic forces of the rotor were computed and the influence of the rotor cone angle on the lateral force and yaw moment is determined. The rotor cone angle of the turbine was changed to values from −6° up to 12° while all other properties remain the same. A negative cone angle inclines the blades in upwind direction while a positive cone angle inclines in downwind direction. Each rotor configuration was simulated with yaw misalignments ranging from 0° up to 45° and with a wind velocity of 10.5 m s^{-1}. It's important to emphasize

that the direction of the aerodynamic force on the rotor acts mainly in axial direction, even at large oblique flows. The rotor force vector does not act in wind direction as it is sometimes incorrectly presumed.

The lateral force and yaw moment on the rotor have large oscillation amplitudes, especially with increasing misalignment angles. These oscillations are induced by the rotor rotation and are related to the blade frequency. A three-bladed configuration would produce forces with higher frequency but lower amplitude. The mean values of lateral force and yaw moment at tower top are shown in Figure 7. Both, lateral force and yaw moment, are relativized to the thrust (815 kN) or torque (3.9 MN m) of the design configuration with 9° cone angle and axial inflow. The lateral force is relatively small compared to the axial (thrust) force, but depends significantly on the rotor cone angle. A downwind cone angle of 9° leads to three times larger lateral force than upwind cone angles (−6° and −3°). However, the lateral force remains small compared to the thrust force. The yaw moment at tower top also increases with larger downwind cone angles. With a cone angle of 9° it is around twice as large as without any rotor cone for misalignment angles of 15° and 30°. The cone angle has little influence on power of the turbine. Compared to the design cone angle of 9° a power loss of around 2 % was calculated for −6° and 12° cone angle.

4.2. Separate yaw moments

A comparison of the mean yaw moments at the position of the SPM is shown in Figure 8. In this case, platform, tower and rotor are simulated separately to obtain their influence independently. The rotor cone angle is set to the design value of 9°. All values are mean values with a wind velocity of $10.5\,\mathrm{m\,s^{-1}}$ or current velocity $0.5\,\mathrm{m\,s^{-1}}$, respectively. Also here the yaw moment is relativized to the rotor torque with axial inflow (3.9 MN m). The turret buoy of the SPM is placed 68 m in front of the tower top, which leads to a large lever arm of the lateral forces induced by rotor and tower. A large lever arm is helpful to dominate the hydrodynamic force. The yaw moment of the rotor itself is nearly the same as the platform moment. Without any tower forces, this would result in misalignment angles that are half the offset angle of wind and sea current. It is essential to reduce the misalignment to a minimum and therefore a large airfoil-shaped tower was designed at the presented platform. The tower has an airfoil area of $740\,\mathrm{m^2}$ and each strut an area of $279\,\mathrm{m^2}$. These large airfoils substantially increase the self-aligning moments of the platform.

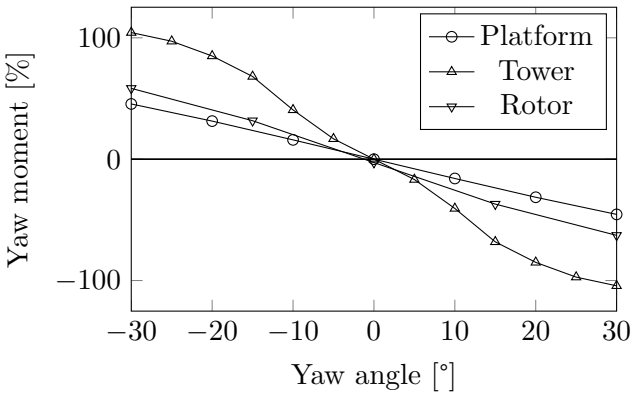

Figure 8. Yaw moments of platform, tower and rotor at center of the SPM calculated separately relativized to the rotor torque with axial inflow.

4.3. Steady state misalignment

The steady alignment of the platform in the presence of sea current is crucial for a self-aligning platform design. In order to obtain an approximation of misalignment angles and expected power loss the full platform with operating wind turbine has been simulated with different sea current velocities and wind-current offset angles. The turbine operation is limited to partial load and the sea current varies from $0.1\,\mathrm{m\,s^{-1}}$ to $0.5\,\mathrm{m\,s^{-1}}$. Offset angles of 30°, 60° and 90° are applied. The mean values over 200 s after transient effects have vanished are shown in Figure 9. Misalignment angles of the platform are given in the first row. The second row shows the

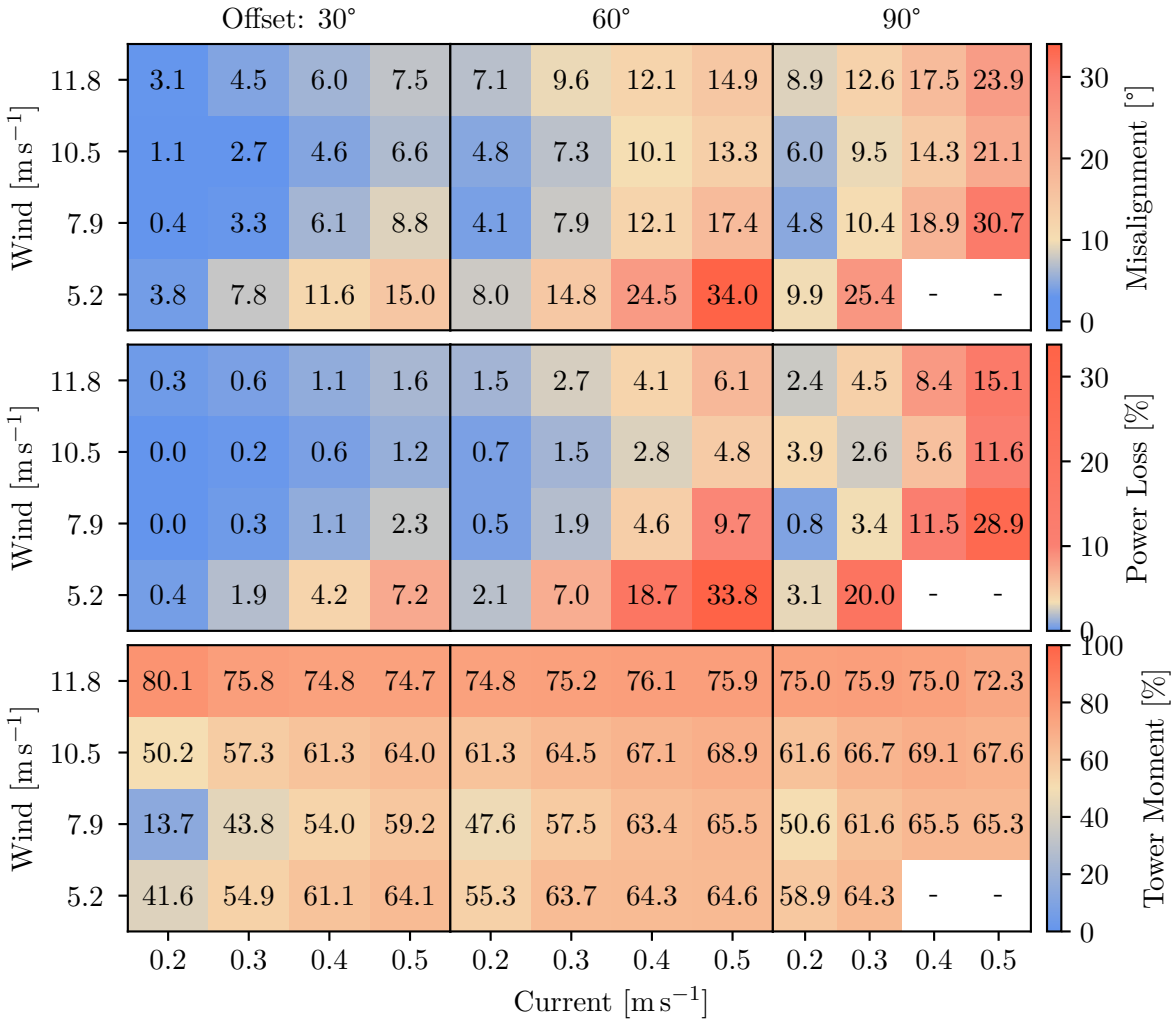

Figure 9. Steady state mean values under wind-current offset.

power loss of the turbine relativized to a wind and current direction of 0°. In the last row, the importance of the airfoil-shaped tower and its aerodynamic lift forces under oblique inflow is shown by the relative part of the tower moment on the total aerodynamic yaw moment of rotor and tower.

Current velocities below 0.3 m s^{-1} lead to misalignment angles below 10° in most cases. Only if the wind velocity is 5.2 m s^{-1}, the angle is considerably larger. A current of 0.5 m s^{-1} with offset angles of 30° or 60° results in higher misalignment angels. In general, the yaw misalignment decreases with increasing wind velocity. At a wind velocity of 11.8 m s^{-1} a small increase is noticeable. This phenomenon is caused by the waves and heeling moments. The wave energy of the seaway increases with wind speed and the wave propagation is orientated with the current direction, see above. Mainly four heeling moments act on the platform. The heeling moment due to the rotor torque is depending on the axial wind velocity. A counteracting heeling moment is induced by the sideways shift of the COG, see above. The tower induces a heeling moment depending on the wind velocity when the platform is not aligned with the wind. Another heeling moment is induced by the current drag at the mooring point when the platform is not aligned with the current. If the total heeling moment is not balanced, the rotor thrust acts with a small

lever arm and thus induces a yaw moment at the SPM. In this case it is best balanced at a wind velocity of $10.5\,\mathrm{m\,s^{-1}}$. Positive heel angles occur at wind velocities of $11.8\,\mathrm{m\,s^{-1}}$ and lead to misaligning moments. Lower wind velocities result in negative heel angles which lead to aligning moments. However, the result would be different if the offset of wind and current is opposite.

The power loss increases strongly when the misalignment angle exceeds 10°. Conventional yaw controllers usually respond on mean yaw errors above 10°. Hence, current velocities up to $0.3\,\mathrm{m\,s^{-1}}$ will result in comparable energy output. The yaw moment caused by the airfoil-shaped tower shows significant influence on the self-aligning mechanism in most cases, especially at high wind or current velocities. It emphasizes the importance of maximizing the yawing moments additional to the rotor in order to minimize the misalignment in the presence of a sea current. At wind speeds above nominal conditions, the proportion of the tower force will increase further because of the quadratic dependence on the relative velocity. The rotor forces instead will be reduced due to blade pitching.

5. Conclusions

Beginning with the rotor forces, it has been shown that even at large misalignment angles, the lateral force is multiple times smaller than the thrust force. The aerodynamic force on the rotor does not act in wind direction and thus does not induce large yaw moments when the rotor is not aligned with the wind. This result is not surprising but is of major importance when designing a self-aligning platform.

The cone angle analysis has shown significant influence of the rotor cone angle on the lateral force and yaw moment. In order to increase the self-aligning moment of the rotor, large downwind cone angles are essential. Such cone angles are only feasible on downwind turbines. A negative cone angle, which is necessary on upwind turbines, does not provide significant yaw moment. Another possibility to increase the self-aligning rotor forces could be an individual blade pitch control where blades are pitched individually, dependent on the rotor angular position. When a blade is directed into the wind, its thrust must be increased, and when it's directed away from the wind, the thrust must be reduced. However, this would no longer be passive self-aligning.

On a passive system other sources of yaw moments are required. At the presented platform design, the tower is used to generate large self-aligning moments. The airfoil-shaped hull is mounted around a supporting main structure and could be designed depending on the expected current at the offshore location. A failure due to the large tower area could happen in case of a side gust. This has not been analyzed yet. If such events can happen, depends on the location. With moderate sea current, the platform will follow the wind direction, especially at high wind velocities even when the turbine is not operating.

The sea current has a major influence on the self-aligning capability. A good steady alignment could be shown for current velocities up to $0.3\,\mathrm{m\,s^{-1}}$. With yaw errors up to 10°, the misalignment is comparable to conventional turbine design with a yaw system that operates on ten minute mean values of the wind direction. The power loss was estimated to be up to 5 % in comparison to an aligned platform. However, a current velocity above $0.3\,\mathrm{m\,s^{-1}}$ could result in large misalignment angles. It would then be necessary to increase the self-aligning moments by additional techniques like a flap on the tower or individual blade pitch. Therefore, it is important to quantify the current velocity and offset angles at the location in advance to determine the feasibility of the passive self-aligning platform.

Acknowledgments
The authors kindly thank the Federal Ministry for Economic Affairs and Energy of Germany (BMWi) for financially supporting the HySToH project [03SX409A-F]. The authors also kindly thank our project partners CRUSE Offshore GmbH, aerodyn engineering gmbh, JÖRSS – BLUNCK – ORDEMANN GmbH, DNV GL and the Institute for Ship Structural Design and Analysis at the Hamburg University of Technology for the excellent cooperation.

References
[1] Netzband S, Schulz C W, Göttsche U, González D F and Abdel-Maksoud M 2018 *Ship Technology Research* **65** 123–136 ISSN 0937-7255
[2] Netzband S, Schulz C W and Abdel-Maksoud M 2020 *Ship Technology Research* **67** 15–25 ISSN 0937-7255
[3] Verelst D R S, Larsen T J and van Wingerden J W 2014 *Journal of Physics: Conference Series* **555** 012103 ISSN 1742-6588
[4] Kress C, Chokani N and Abhari R 2016 *Renewable Energy* **89** 543–551 ISSN 09601481
[5] Schulz C W, Wieczorek K, Netzband S and Abdel-Maksoud M 2019 *Journal of Physics: Conference Series* **1356** 012018 ISSN 1742-6588, 1742-6596
[6] Wanke G, Hansen M H and Larsen T J 2018 Qualitative yaw stability analysis of free-yawing downwind turbines Preprint Aerodynamics and hydrodynamics
[7] Bauer M and Abdel-Maksoud M 2012 A 3-D Potential Based Boundary Element Method for Modelling and Simulation of Marine Propeller Flows *7th Vienna International Conference on Mathematical Modelling* vol 7 (Vienna) pp 1179–1184 ISSN 1474-6670
[8] Hundemer J 2013 *Entwicklung Eines Verfahrens Zur Berechnung Der Instationären Potenzialtheoretischen Propellerumströmung* Ph.D. thesis Hamburg University of Technology
[9] Schoop-Zipfel J and Abdel-Maksoud M 2014 Maneuvering in Waves Based on Potential Theory *33rd International Conference on Ocean, Offshore and Arctic Engineering (OMAE2014)* vol 8B (San Francisco)
[10] Katz J and Plotkin A 2004 *Journal of Fluids Engineering* **126** 293 ISSN 00982202
[11] Hall M and Goupee A 2015 *Ocean Engineering* **104** 590–603 ISSN 0029-8018
[12] Sarraf C, Djeridi H, Prothin S and Billard J Y 2010 *Journal of Fluids and Structures* **26** 559–578 ISSN 08899746